Investigation of secondary droplet characteristics produced during wall impact

by

B. Richter[(1)], K. Dullenkopf[(2)], and H.J. Bauer

Lehrstuhl und Institut für Thermische Strömungsmaschinen (ITS)

Universität Karlsruhe

Kaiserstr. 12, 76131 Karlsruhe, Germany

[(1)]E-Mail: boyke.richter@its.uni-karlsruhe.de

[(2)]E-Mail: klaus.dullenkopf@its.uni-karlsruhe.de

ABSTRACT

In numerous technical applications droplet impingement on hot walls is a phenomenon of great importance. During mixture formation inside DISI engines e.g., a huge number of small droplets with high velocity and a typical SMD below 20 µm impinge on a hot wall during fuel injection. The physics of this impingement process is mostly unknown due to the difficulties to gain experimental access. In this publication the impingement of small Isooctane droplets on a hot surface is studied. The emphasis was put on the temporal interaction of successive impingement processes and its influence on secondary droplet size and velocity. Using an image based analysis technique, size and velocity of the droplets are measured coincidently and a visual impression of the impingement situation and the regime is gained additionally. **Fig. 1** exemplarily shows the influence of different time gaps between successive impingement processes on a hot wall heated above the Leidenfrost temperature. At the left side a large time gap leads to almost no interaction. The droplets spread, disintegrate into several secondary droplets which are leaving the wall. At the right side a very small time gap leads to significantly larger secondary droplets and a movement more parallel to the wall.

The intention of this study in the context of the European Research Project DWDIE was to expand the knowledge of interaction processes during droplet wall collision particularly for DISI engines. The demand for theoretical prediction of real spray wall interaction makes the detailed analysis of interaction processes necessary, because the simple superposition of single droplet impingement events doesn't lead to satisfactory results (Tropea and Roisman (2000)).

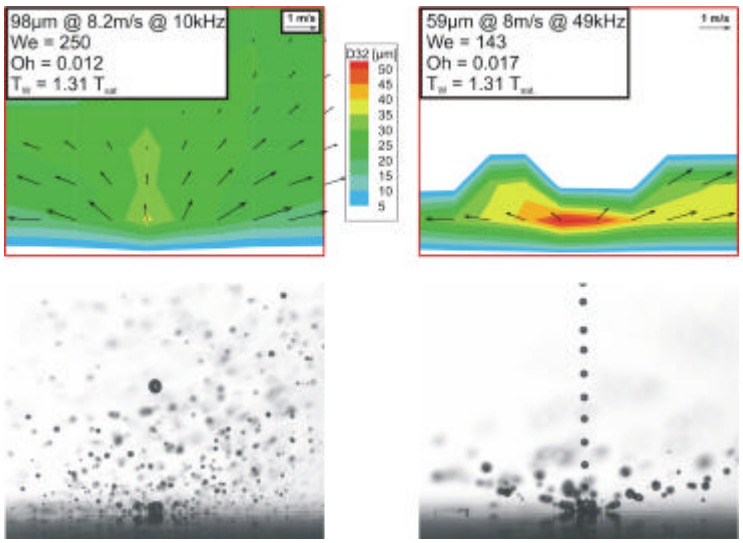

Fig. 1: Influence of impact frequency on secondary droplet production

INTRODUCTION

The modern engine concept of direct injection spark ignition (DISI) engines provides a significant potential for improvements regarding fuel consumption and consequently CO_2 emissions. On the other hand, clearly visible difficulties exist to reach recent standards with respect to the emission of unburned hydrocarbons. This is mainly due to the inhomogeneity of the mixture with local very rich areas in the mixture and pools of liquid fuel on the walls of the combustion chamber. They can be attributed to the interaction phenomena between the droplets of the spray and the walls of the combustion chamber. To improve the emission characteristics of DISI engines exact knowledge of these phenomena and reliable numerical design tools are necessary.

Investigations of the impact of single drops on solid surfaces have been presented in the open literature by various authors. Rioboo et al. (2001) investigated the influence of surface roughness and wettability of the liquid/solid/gas system. They used a Syringe equipped with different precision needles to produce single droplets of a few millimeters in diameter. The impact velocity varied with the height of the needle above the surface. The outcome from the impact was recorded using a CCD camera. By means of single exposure images the regime and small ejected droplets were resolved while multiple exposure images were used to gain an overview of the entire process. Six possible impact regimes were identified and separated in Deposition, Rebound and Partial Rebound, as well as different forms of Splash. The influence of a change of various parameters regarding the primary droplets and the surrounding conditions was presented together with an overview of the sensitivity of the process to a change of these parameters.

For the investigation of the interaction between successive droplet impacts, Yarin and Weiss (1995) used a droplet chain generator and observed the impingement process by means of a camera and a computer based picture processing unit. Using different nozzle diameters the droplet diameter was varied between 70 and 340 µm while the droplet velocity was controlled by the pressure in a reservoir which allowed velocities up to 30 m/s. They derived from their experiments a splashing threshold dependent on the impact frequency and velocity, but independent of the primary droplet size. Furthermore they formulated a model describing the crown formation as a discontinuity in the velocity and film-thickness distributions. The impingement of a droplet chain can be seen as the impact on a partially wetted wall, because the liquid is not removed totally between two impact processes. For completely wetted surfaces, Cossali et al. (1997) identified a Splash-Deposition limit. They used needles of different size to produce single drops with diameters between 2 and 5.5 mm. The impact velocity was determined by varying the needle height and ranged up to 6.5 m/s. The splash was observed and recorded by a camera. As well single images illuminated by a strobe lamp as long exposure images using a laser light sheet for a visualization of the droplet trajectories were obtained. Splashing during the impact of a droplet on a liquid film is characterized by the formation of a crown with emerging jets that disintegrate into secondary droplets. Interdependencies between the number of these jets and the number of secondary droplets were identified and established. Samenfink et al. (1998) analyzed the interaction between droplets and a shear-driven liquid film on the surface, esp. with regard to the secondary droplet characteristics. They used a vibrating orifice droplet chain generator to produce a stream of monosized droplets. The primary droplet size was varied between 100 and 200 µm and the primary droplet velocity between 9 and 20 m/s. From this investigation, a complete set of correlations to calculate the behavior of the secondary droplets was evaluated.

Regarding the impact of droplets on hot surfaces, the main emphasis found in the literature was put on the investigation of the "Leidenfrost point". Bernardin (1996) e.g. performed detailed experiments to study the processes taking place at an impingement under Leidenfrost conditions. The Leidenfrost point is characterized by the immediate formation of a vapor layer that separates the droplet from the wall, if the wall is heated above the Leidenfrost temperature. This means, that the droplet doesn't get in direct contact with the wall during the impingement process. The characteristic outcome of a droplet impact above the Leidenfrost point, also referred to as the Film Boiling regime, was a Rebound. The Rebound in general is a dynamically driven phenomenon. The receding of the liquid disc, in which the primary droplet is deformed during impact, is driven by surface tension forces and damped by contact forces between liquid and wall. If the surface tension forces overweigh the contact forces, the liquid regroups to a distorted droplet and rebounds back from the wall. The size of the secondary droplet is equal to the primary one, only potential evaporation due to an elevated surface temperature can reduce the liquid mass of the droplet. The velocity is lower than the impacting velocity due to momentum loss during deformation of the droplet.

In general various authors published correlations to provide the capability to predict the results of an impingement of a droplet on a solid wall (see e.g. Mundo (1996), Samenfink (1997), Weiss (1993)). Almost any of these correlations were developed using large droplets of pure liquids or mixtures, in order to simulate fuel

properties. Comparing the results of these correlations for the range of conditions and liquid properties relevant for DISI engines, significant deviations become obvious. Concerning the experimental conditions it seems that still not all influencing parameters were taken into account. Therefore, experiments under conditions as close as possible to realistic DISI engines are necessary.

Additionally to the fact that still not one global consistent correlation could be found that includes all necessary influencing parameters and is applicable to DISI conditions, it becomes more and more apparent, that it is not possible to simulate real spray wall interaction by superimposing single droplet impact events (Tropea and Roisman (2000)). This makes it necessary to investigate in detail the interaction between several impingement processes which includes both interaction in time and space. The temporal interaction means that successive droplets impinge at the same location one shortly after the other before the end of the individual impingement process (Yarin and Weiss (1995)). Spatial interaction occurs, when the spreading lamellas of two adjacent droplets collide and interact (Barnes et al. (1999)).

In a current investigation at the ITS the behavior of secondary droplets under near realistic conditions of the DISI engine is analyzed with specialized instrumentation. The investigation of the interaction between several impingement processes should extent the results of single droplet experiments to be more applicable for the prediction of spray wall interaction. Results of the investigation of single droplet impact can be found in Richter et al. (2002 and 2003). The focus of the current publication was mainly put on the temporal interaction of successive droplets of a monodisperse droplet stream.

EXPERIMENTAL SETUP

The basic test rig for the investigation of droplet chain impingement consisted of a droplet generator and a heated wall element. **Fig. 2** shows a schematic overview of the test rig. At the right an image of the global surrounding at the impingement area is presented. The droplet chain passing an LDV measurement volume is clearly visible. The image shows the conditions of the vertical impingement of Isooctane droplets with 80µm in diameter and a velocity of 8.5 m/s on the fine machined wall at a high wall temperature of 489 K.

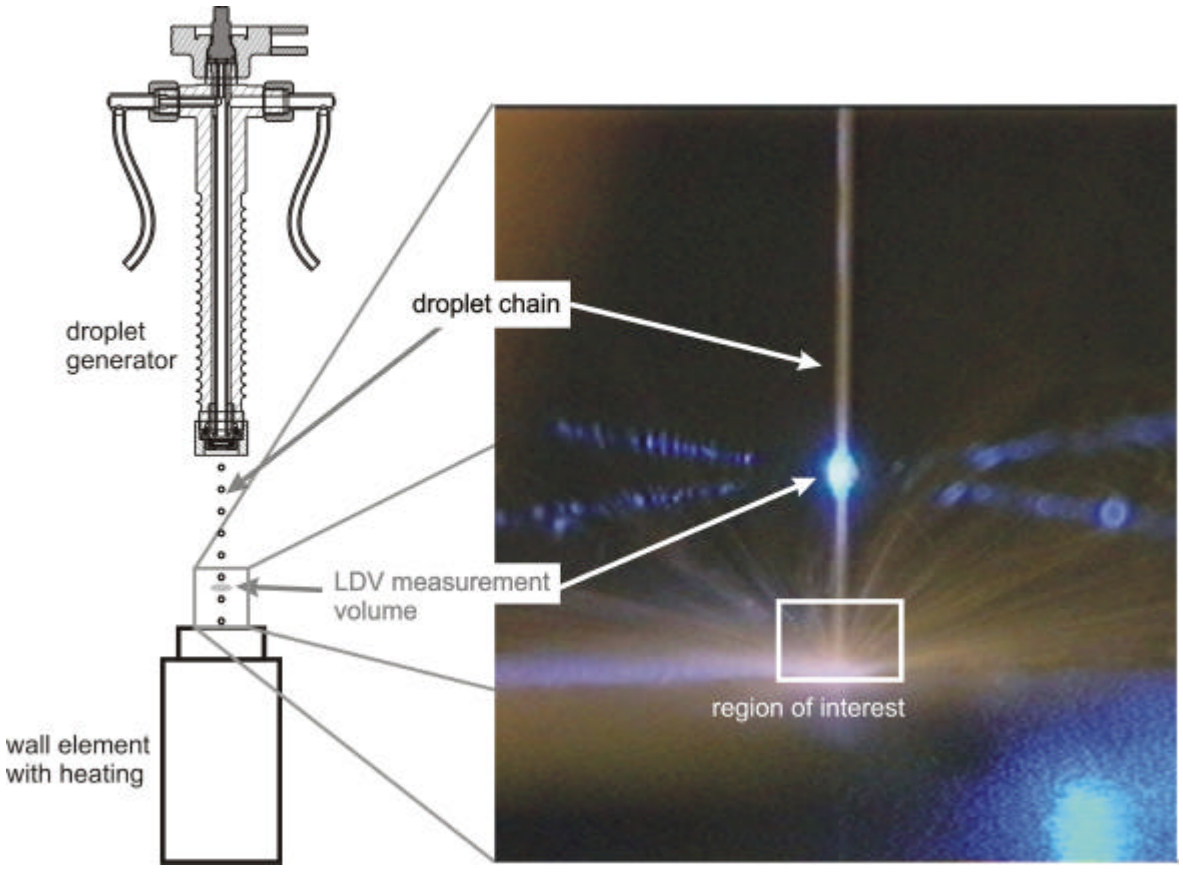

Fig. 2: Schematic overview of the complete test rig for the investigation of droplet chain impingement

The droplet generator was a vibrating orifice droplet generator using a piezoelectric oscillator to excite a liquid jet to disintegrate regularly into equally spaced and sized droplets. The minimum droplet size was mainly restricted by the manufacturing of the orifice and the control of the jet disintegration. The orifice used had a diameter of 25 µm and the size of the droplets ranged between 60 and 100 µm depending on the relation between liquid feed pressure and the excitation frequency (see also **Tab. 1**). Because these sizes represent the range of the larger droplets occurring in real DISI sprays, no further variation which could only increase the droplet size by using a larger orifice was performed. The piezo oscillator of the droplet generator was driven by an AC square wave signal, whereas the frequency of this signal was optimized to receive periodical droplet disintegration. The generator was fed by a pressurized reservoir. The pressure drop over the orifice controlled the velocity of the droplets produced.

To adjust the location of the droplet impact and to continuously check the primary droplet velocity and uniformity the measurement volume of a 1D LDV was placed directly above the wall element. This device provided additionally the possibility to synchronize the measurement system with the impingement process and enables a phase resolved characterization of the process. The wall element was cut from a real engine piston representing real surface roughness and material. It was fixed on a copper block that was heated by a heating cartridge and the surface temperature was controlled by a closed loop regulator and a thermocouple mounted directly beneath the impact location in the aluminum wall element.

Tab. 1 summarizes the boundary conditions of the presented experiments. The main variation parameters were the wall temperature and the spacing parameter between successive droplets. **Tab. 2** lists the liquid properties of Isooctane used for all experiments.

Tab. 1: Boundary conditions for droplet chain experiments

Parameter	Experimental range
Test fluid	Isooctane (properties see **Tab. 2**)
Primary droplet size	between 60 and 100 µm, depending on pressure/excitation frequency relation
Primary droplet velocity	3.8 m/s and 7.8 m/s
Spacing parameter	between 6 and 51 kHz
Wall temperature	1.02, 1.10, 1.17, 1.24, and 1.31 x $T_W/T_{sat.}$ and the crit. Temp. of Isooctane
Surface roughness	R_z = 5.8 µm, R_a = 1.0 µm

Tab. 2: Liquid properties of the test fluid

Liquid	$T_{sat.}$ [K]	$T_{crit.}$ [K]	Density [kg/m³]	Surface Tension [N/m]	Dyn. Viscosity [Pa s]
Isooctane	372.4	543.8	688.8	0.0182	0.466 x 10^{-3}

The task of investigating secondary droplet size and velocity distributions includes high demands on the experiment and the measurement system. To study the morphology of the impingement process and to understand the outcome visual access is necessary. The impingement process was illuminated from the background and observed using a CCD camera equipped with a long distance microscope. To investigate the velocities of the secondary droplets two different techniques are applicable; on the one hand the PIV technique which only resolves the velocity of the droplets and needs additional experiments to achieve the necessary droplet sizes, on the other hand the image analysis technique which allows the determination of size and velocity of the droplets coincidently.

To demonstrate the basic differences between the two techniques with regard on the acquisition **Fig. 3** shows two exposures of a chain of monosized Isooctane droplets impinging on a heated aluminum surface. The primary droplet size is 80 µm and the velocity is 8 m/s, while the distance between successive droplets is 430 µm. The wall is heated to 490 K which is 31 % above the saturation temperature of Isooctane. Regarding these conditions,

the process lies in a regime where film boiling occurs (refer to e.g. Cossali et al. (2002), Bernardin (1996)). Because the wall temperature is above Leidenfrost conditions no direct contact between liquid and wall takes place. The droplets spread along the wall, disintegrate into several secondary droplets which are leaving the wall again with certain size and trajectories.

The left side of **Fig. 3** shows an example of a backlight image. The area has a size of 2.3 x 1.8 mm and is illuminated by means of a fluorescent liquid pumped by a Nd:YAG laser. Using this setup an ideal homogeneous background illumination with two very short light pulses of app. 25 - 35 ns and an adjustable delay of 1 - several 100 µs in between could be achieved. The right side shows a raw PIV frame under similar experimental conditions, but the image size is larger (6.2 x 4.9 mm).

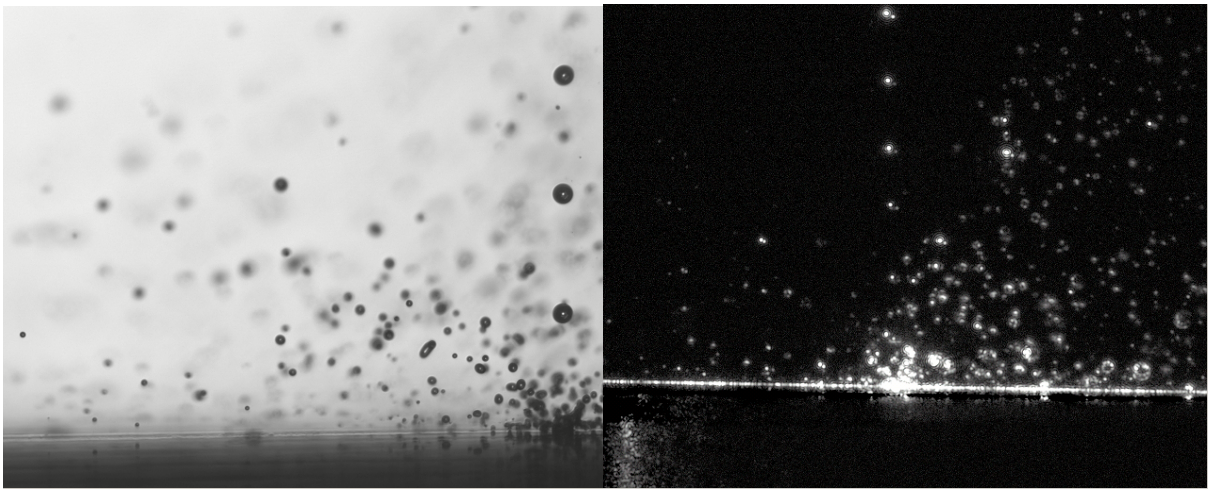

Fig. 3: Backlight and PIV image of a droplet chain impingement on a hot surface

Both measurement techniques have their advantages and limitations. PIV provides well known accuracy and robustness of the velocity evaluation. But the micron-scale investigation with sparse distributed liquid droplets instead of equally distributed and sized tracer particles causes significant difficulties. Additionally the significant variations in droplet size and velocity over each image area prevent the occurrence of sharp peaks in the correlation function. Furthermore, the larger droplets are represented by two glare points and a light ring on their surface, while in case of small droplets these glare points overlap to a Gaussian distribution of the scattered light that is normally encountered in PIV measurements and the evaluation algorithm is optimized for.

Image analysis provides quantitative and coincident information on droplet size and velocity. Additionally the impingement process and the regime can be clearly identified from the images. Each droplet is identified individually, so no limitations regarding velocity gradients or too few droplets are present. But the evaluation algorithm suffers from contrast variations in the illumination due to blurred droplets which are out of focus. Furthermore difficulties with overlapping droplet images exist which leads to a maximum of droplet density that can be evaluated. Another restriction is a slight dependence of the calculated droplet sizes on thresholds which have to fit to all droplets in each frame. Furthermore, the smallest detectable droplet diameter was found to be app. 2-3 pixel whereby the real sizes then depend on the magnification.

Summarizing, it has to be stated that PIV is only applicable to an investigation of the presented phenomena under special conditions. Especially the significant variation of the sizes of the secondary droplets and the often size dependent velocities limit the application of this measurement technique. Finally PIV is only able to provide droplet velocities and suffers in the vicinity of the primary droplets from their strong signal intensity. Image analysis is only limited to low droplet density but is able to measure size and velocity of the droplets coincidently. It is shown by the presented experiments that the image based droplet evaluation is extremely suitable for the investigation of droplet wall collision.

RESULTS AND DISCUSSION

As already mentioned, the main emphasis of the current investigation was put on the temporal interaction of successive droplet impingement processes regarding the secondary droplet characteristics. **Fig. 4** shows the dependence of the velocities and sizes of the secondary droplets produced during wall collision on the wall

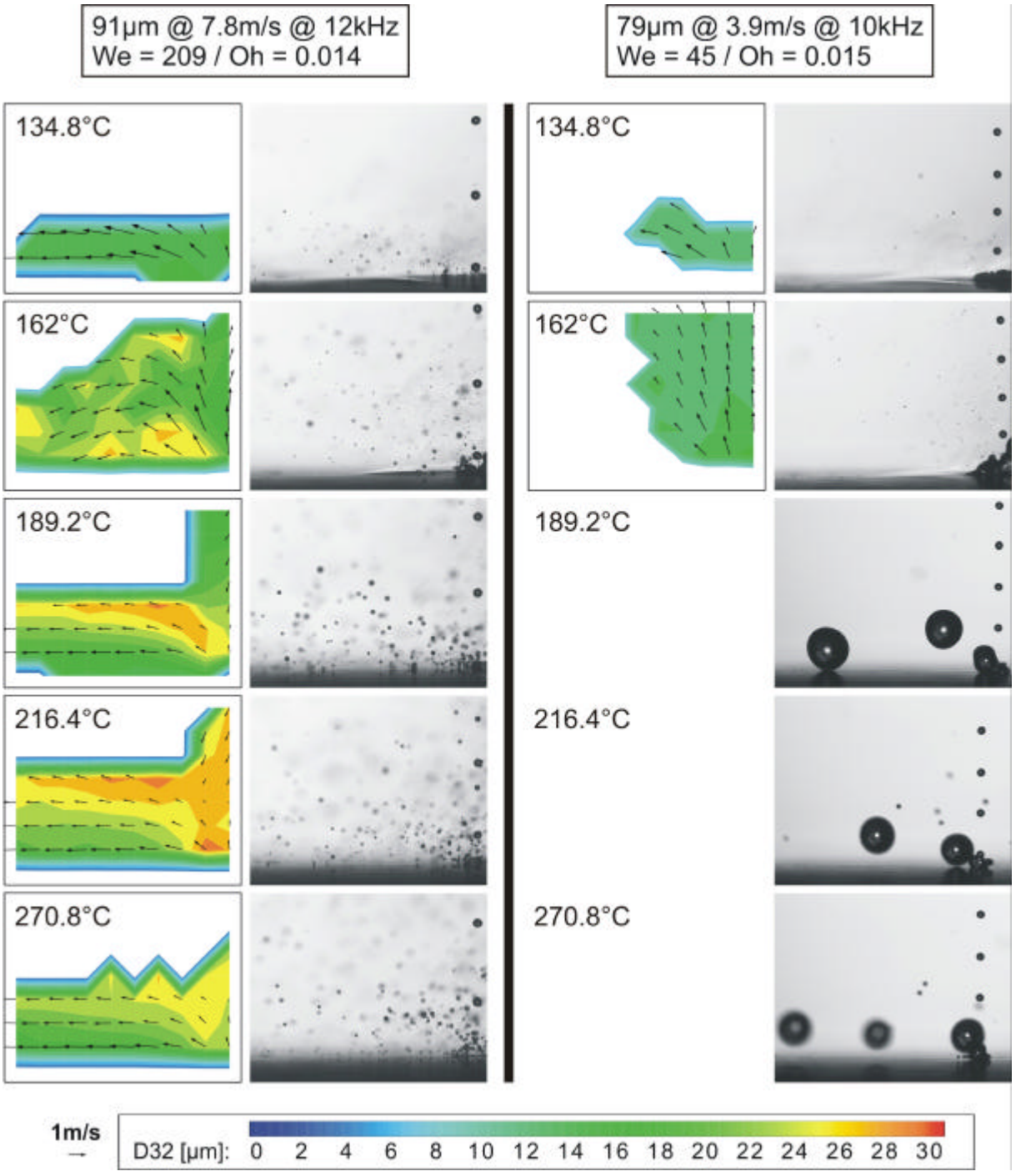

Fig. 4: Variation of wall temperature and primary droplet velocity – Influence on regime and secondary droplet size and velocity

temperature and the primary droplet velocity. The figure is divided into two main groups of images by different primary droplet chains. The left two columns present droplets with diameter of 91 µm hitting the wall with a velocity of 7.8 m/s and a frequency of 12 kHz which corresponds to a distance between droplets of 650 µm in space and 83 µs in time. The rows of images represent different wall temperatures.

The experiments were started with a wall temperature of 107°C which is only 2% above the saturation temperature of Isooctane and 70% of the critical temperature. At this low wall temperature no secondary droplets were produced, therefore no results are included in the figure. It additionally shows that the dynamic conditions of the impact lead to deposition when no heat transfer from the wall influences the liquid on the wall. But already an increase of the wall temperature to 134°C leads to significant occurrence of very small secondary droplets as shown in the first figure of the left column in **Fig. 4**. The next rows of figures show an increase of the

wall temperature in steps of 5% of the critical temperature. The lowest figures show the impingement on the wall heated to the critical temperature of Isooctane itself.

The right two columns of **Fig. 4** show similar conditions but for a lower primary droplet velocity of 3.9 m/s, primary droplet size of 79 µm and an impingement frequency of 10 kHz which corresponds to a distance between droplets of 380 µm in space and 100 µs in time. Again a wall temperature below 134.8°C leads to deposition without the occurrence of secondary droplets. In the first row a wall temperature of 134.8°C is shown and small secondary droplets are visible in the vicinity of the impingement location. To the left of each image in **Fig. 4** a vector plot of the movement of the secondary droplets is presented whereby the colors in the back of the vector plots correspond to the SMD of the secondary droplets. These plots represent the average of 500 single images. For a wall temperature of 134.8°C slightly smaller droplets (SMD of 11 µm) are produced in case of the lower primary droplet velocity (right side) compared to the higher primary droplet velocity (left side, SMD of 14 µm). In both cases bubble boiling occurs which means that vapor bubbles grow inside the liquid pool at the impingement location which collapse and form these small droplets. The higher momentum of the primary droplets in the latter case leads to stronger disturbances and to the formation of waves which cause a stronger movement of the droplets parallel to the wall because the secondary droplets are driven away by the energy of the impact of the following droplets. This process is even more evident for a higher wall temperature of 162°C shown in the second row of **Fig. 4**. The case of lower primary droplet velocity (right side) shows mainly an upward movement of the small secondary droplets. The collapse of vapor bubbles tends to spread the droplets radially equally distributed but the wall parallel movement is hindered by the surrounding liquid leading to the preference of the upward movement. For the higher primary droplet velocity some larger droplets occur which are pulled out of the liquid due to the disturbances caused by the impact. This also drives the secondary droplets radially away from the impingement location parallel to the wall.

A further increase of the wall temperature to 189.2°C causes significant differences in secondary droplet production esp. for the lower primary droplet velocity (see **Fig. 4** right side). No small secondary droplets are visible but some very large ones (300 µm and above) emerge from the impact location. This effect can be attributed to the Leidenfrost phenomenon, which means that for a primary droplet velocity of 3.8 m/s and primary droplet size of 79 µm the Leidenfrost temperature lies between 162°C and 189°C. Above the Leidenfrost temperature the liquid doesn't get in touch with the surface any more. Because of this no vapor bubbles grow inside the liquid, because the heat transfer from the wall to the liquid is strongly reduced by a vapor layer between them. Without collapsing vapor bubbles no small droplets emerge, but the liquid grows at the impact location fed by the impinging droplets. When the liquid mass exceeds a critical value a large droplet separates and moves slowly away. This phenomenon above Leidenfrost does not depend on the wall temperature and consequently doesn't change with a further increase of the wall temperature (three lower rows of **Fig. 4**).

This process of large droplet formation doesn't occur for a higher primary droplet momentum (see **Fig. 4**, left side). Due to the stronger dynamic interaction with the wall, the liquid spreads further during impingement and disintegrates into several droplets instead of growing to a large droplet. Due to this the Leidenfrost temperature can't be identified directly from the impingement process as in the previously discussed case. But still some changes in the behavior of the secondary droplets can be identified when increasing the wall temperature from 162°C to 189.2°C. Slightly larger droplets can be found in the image and the upward movement of the droplets disappeared almost completely. A strong movement of the droplets parallel to the wall becomes evident which can also be clearly seen in a very similar manner for the next two wall temperatures of 216.4°C and 270.8°C. This leads to the assumption that the Leidenfrost temperature lies between 162°C and 189°C also for the higher primary droplet velocity for which some evidence can be found by the presented results, but which can't be stated as clearly as in case of the lower primary droplet velocity. Another interesting effect of an increase in the wall parallel velocity component can be identified from the velocity distributions at the three highest wall temperatures. This behavior can be explained by lower friction between the liquid and the wall with increasing wall temperature caused by an increase in the strength of the vapor layer separating the liquid from the wall. But this also means that there is still a difference in wall contact between these wall temperatures.

Fig. 4 presents an overview of the dependence of the secondary droplets on the primary droplet velocity and the wall temperature. **Fig. 5** shows similar arranged results of a variation of the impact frequency without changing the primary droplet velocity. Due to the dependence of the excitation frequency of the droplet generator the primary droplet sizes could not be kept constant, but the impinging liquid mass flow stays the same. For all impingement frequencies the wall temperature was 216.4°C which is definitely above the Leidenfrost temperature.

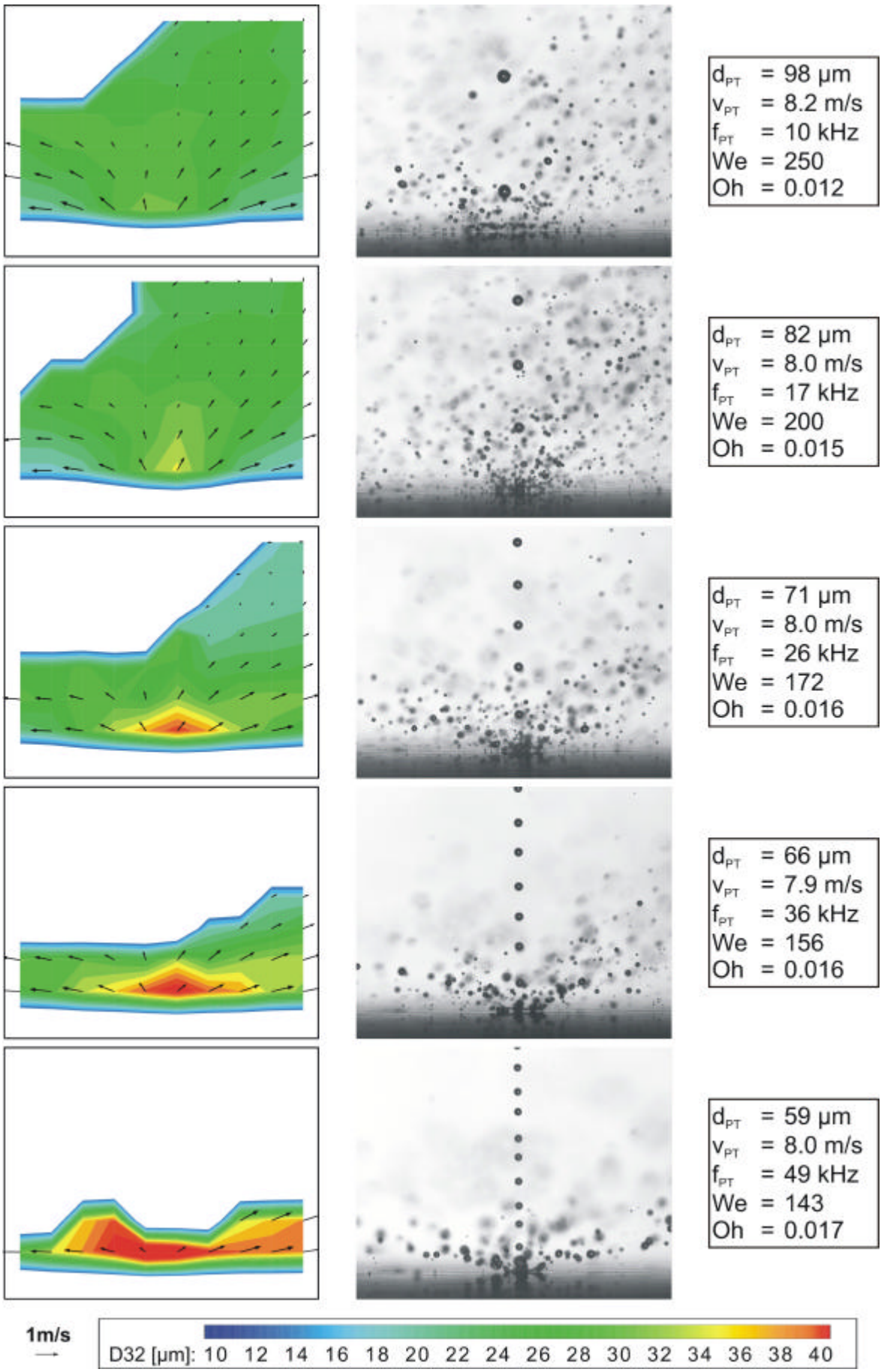

Fig. 5: Variation of temporal distance between successive impingement processes

The first case shows an impingement frequency of 10 kHz which corresponds to a distance of 820 µm in space and 100 µs in time. The image shows a flat liquid disc above the wall which is the lamella of the just impacted droplet that levitated from the wall and disintegrated into several secondary droplets that are leaving the impingement location. This means that the impact process is finished before the next droplet arrives and thus no interaction between successive impingement processes takes place. Increasing the impingement frequency to 17 kHz which corresponds to a distance of 470 µm in space and 59 µs in time shortens the time between successive impact processes significantly but still doesn't lead to continuous interaction. Only a frequency of 26 kHz (307 µm / 38 µs) shortens the time gap to that extent, that the impingement process is not finished until the following droplet arrives. Further increase of the frequency to 36 kHz (220 µm / 28 µs) and 49 kHz (160 µm / 20 µs) leads to an interaction more and more early in the impingement process of the individual droplet.

Comparing the secondary droplet characteristics for the different impingement frequencies shows a continuous increase of the secondary droplet sizes. As summarized in **Fig. 6**, the global SMD increases from 25 µm to 42 µm, while the wall parallel velocity component increases from 0.4 m/s to 0.75 m/s. Furthermore the secondary droplets are distributed almost all over the image for the first two cases without interaction. This situation changes with the degree of interaction to a strong movement of the droplets almost parallel to the wall which causes the occurrence of droplets only near the wall. This leads to the assumption that the higher degree of interaction in case of higher impingement frequency leads to the formation of waves that forces the liquid to disintegrate at the tip of the lamella. Thus the secondary droplets are driven outwards by the following impact process instead of the self generated disintegration at the end of the spreading process in case without interaction.

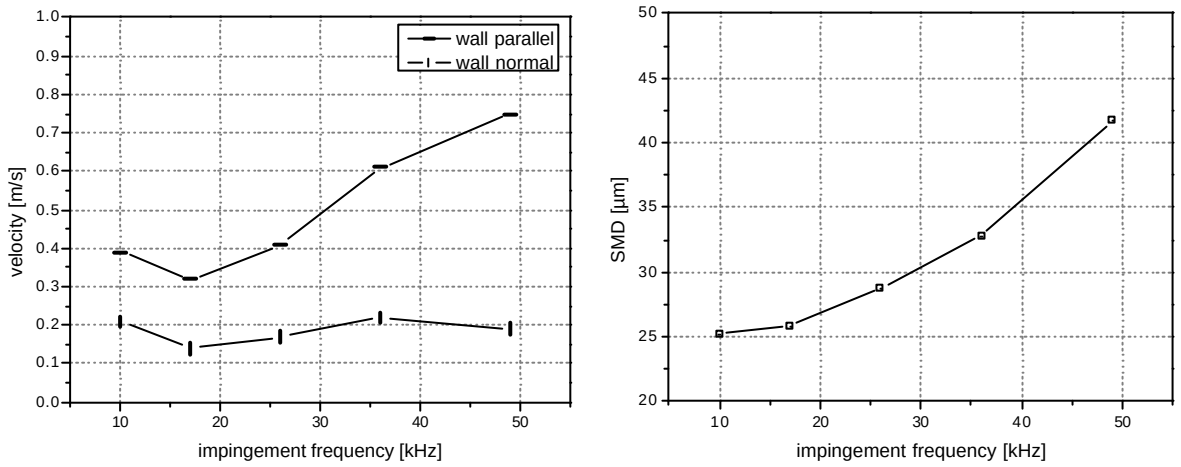

Fig. 6: Secondary droplet velocities and sizes dependent on the impingement frequency

OUTLOOK

As already mentioned additionally to the temporal interaction detailed knowledge of the spatial interaction between adjacent impingement processes is crucial for predicting real spray wall interaction. Using a specialized orifice with several holes, multiple droplet chains can be produced and the interaction of their impact can be investigated. **Fig. 7** shows exemplarily the impingement of three adjacent droplet chains having a distance of 300 µm between them. The primary droplet size was 65 µm and the primary droplet velocity 8 m/s. The left side of the figure shows a view parallel and the right side perpendicular to the three chains. Consequently the droplets that are in focus in the left image are mainly produced between adjacent chains and thus represent the outcome of the interaction of the spreading lamellas. While in the right image the droplets in focus are mainly produced from the rightmost chain towards the free area without an adjacent chain.

It becomes evident from the pictures and the size distributions of the secondary droplets which are shown above the pictures in **Fig. 7** that the interaction of the lamellas leads to the production of significantly larger droplets compared to the undisturbed impingement without interaction. Similar results are reported from Cossali et al. (2003) who investigated the adjacent impingement of three separated millimetric drops and found the occurrence of uprising jets due to the lamella interaction which disintegrate into larger droplets.

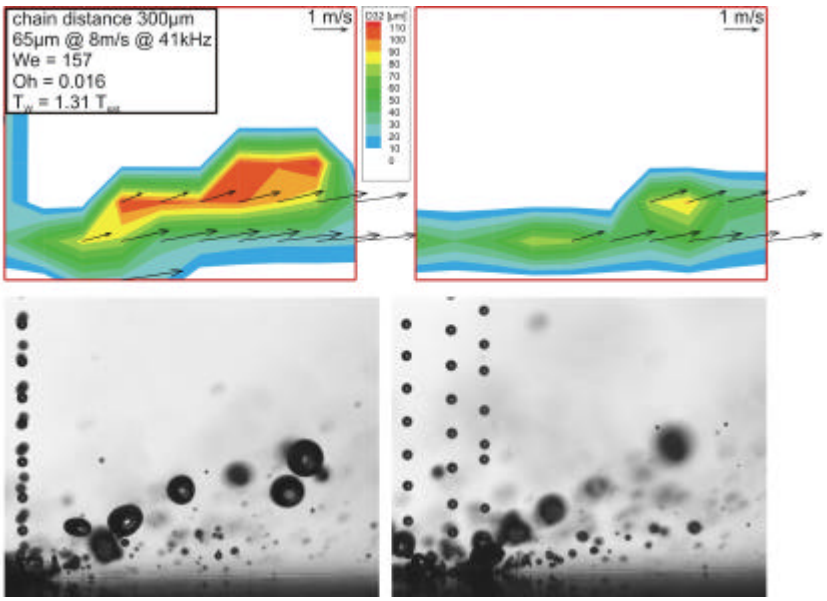

Fig. 7: Spatial interaction between impingement leads to differences in secondary droplet sizes formed between neighboring impingement locations (left side) and formed without interaction (right side)

Further investigations of the spatial interaction of impingement processes under realistic conditions are necessary and are currently performed. The combination of single droplet, single droplet chain and multiple droplet chain impact under similar impingement conditions lead to an improved knowledge of the real spray wall interaction. Still great effort is necessary to complete the global understanding of the processes involved in these phenomena and to build up reliable correlations that allow the prediction of spray wall interaction inside DISI engines.

SUMMARY

The temporal interaction of the impingement process of Isooctane droplets on a hot piston surface was investigated under conditions close to them occurring inside real DISI engines. The very small droplets make high demands on the measurement system and the control of the experiment. It could be shown that using laser based double pulse illumination and a high resolution double shutter CCD camera, high quality images can be obtained. Image analysis technique turned out to be a valuable tool providing coincident measurement of droplet size and velocity. The focus of the investigation was put on the influence of the wall temperature, the primary droplet velocity and the impingement frequency on the secondary droplet sizes and velocities. It was found, that below 134°C no secondary droplets are produced during the impingement process. For a low primary droplet velocity of 3.8 m/s the Leidenfrost temperature could be identified to be between 162°C and 189°C. Some evidence could be found that the Leidenfrost temperature is in a similar range even for higher primary droplet velocities. Furthermore a strong dependence of the movement and the sizes of the secondary droplets on the impingement frequency could be derived. With increasing frequency and thus increasing degree of interaction the secondary droplets are getting larger and are moving more parallel to the wall instead of leaving the impingement area perpendicular to the wall. Overall it can be stated that the temporal interaction has a significant influence on the secondary droplet characteristics.

ACKNOWLEDGMENT

The authors appreciate the financial support of the European Commission through project DWDIE (5th framework program) and state their solely responsibility and that the content of the presented work doesn't represent the opinion of the European Community.

REFERENCES

Barnes, H.A., Hardalupas, Y., Taylor, A.M.K.P. and Wilkins, J.H. (1999), *"An investigation of the interaction between two adjacent impinging droplets"*, 15th ILASS Conference, Toulouse, France

Bernardin, J.D. (1996). *"Leidenfrost Point and Film Boiling Heat Transfer of Single Droplets and Sprays"*, PhD-Thesis, Purdue University

Cossali, G. E., Coghe, A., and Marengo, M. (1997), *"The Impact of a Single Drop on a Wetted Solid Surface"*, Experiments in Fluids, Vol. 22, pp. 463-472

Cossali, G.E., Marengo, M., Santini, M., and Watanabe, J. (2002). *"Secondary Droplet Atomisation from Single Drop Impact on Heated Surfaces"*, ILASS-Europe, Zaragoza

Cossali, G.E., Marengo, M., and Santini, M. (2003). *"Multiple drop impact on heated surface"*, 9th ICLASS, Sorrento, Italy

Mundo, C. (1996), *"Zur Sekundärzerstäubung newtonscher Fluide an Oberflächen"*, University of Erlangen-Nürnberg, PhD-Thesis

Richter, B., Dullenkopf, K. and Wittig, S. (2002), "Wandaufprall von Einzeltropfen unter motornahen Bedingungen von Di-Ottomotoren", Spray Conference, Freiberg, Germany

Richter, B., Dullenkopf, K. and Wittig, S. (2003), "Wall impact of single droplets under conditions of DISI-Engines", 9th Int. Conf. on Liquid Atomization and Spray Systems; Sorrento, Italy

Rioboo, R., Tropea, C., and Marengo, M. (2001), *"Outcomes from a Drop Impact on Solid Surfaces"*, Atomization and Sprays, Vol. 11, pp. 155-165

Samenfink, W. (1997), *"Grundlegende Untersuchungen zur Tropfeninteraktion mit schubspannungsgetriebenen Wandfilmen"*, University of Karlsruhe, PhD-Thesis

Samenfink, W., Elsäßer, A., Dullenkopf, K., and Wittig, S. (1998), *"Droplet Interaction with Shear-Driven Liquid Films: Analysis of the Secondary Droplet Characteristics"*, ILASS-Europe, Manchester

Tropea, C. and Roisman, I.V. (2000), *"Modeling of spray impact on solid surfaces"*, Atomization and Sprays, Vol. 10, pp. 387-408

Weiss, D.D. (1993), *"Periodischer Aufprall monodisperser Tropfen gleicher Geschwindigkeit auf feste Oberflächen"*, University of Göttingen, PhD-Thesis

Yarin, A.L. and Weiss, D.A. (1995), *"Impact of drops on solid surfaces: self-similar capillary waves, and splashing as a new type of kinematic discontinuity"*, Journal of Fluid Mechanics, Vol. 283, pp. 141-173